Comparison of Heat Transfer and Pressure Drop Characteristics of Heat Exchangers Having Plain Fins Under Dry and Wet Conditions

Nae-Hyun Kim†, Tae-Ryong Sin*, Eung-Ryul Lee*

Department of Mechanical Engineering, University of Incheon, Incheon 402-749, Korea

**Graduate School, University of Incheon, Incheon 402-749, Korea*

Key words: Wet surface, Dry surface, Heat transfer coefficient, Plain fin, Heat exchanger, Pressure drop

ABSTRACT: In this study, dry and wet surface pressure drop and heat transfer characteristics of heat exchangers having plain fins were investigated. Nine samples having different fin pitches and rows were tested. The wet surface heat transfer coefficient was reduced from experimental data using enthalpy-potential method. The wet surface heat transfer coefficients were approximately equal to the dry surface values except for one row configuration. For one row configuration, the wet surface heat transfer coefficients were approximately 30% lower than the dry surface values. For the pressure drop, the wet surface yielded approximately 30 % higher values compared with the dry surface counterpart. Data were compared with existing correlations.

Nomenclature

A : heat transfer area [m^2]
b : slope of the enthalpy-temperature curve at saturation condition [kJ/kgK]
c_p : specific heat [kJ/kgK]
D : tube outside diameter [m]
f : friction factor [-]
h : heat transfer coefficient [W/m^2K]
i : enthalpy [kJ/kg]
j : Colburn j factor [-]
k : thermal conductivity [W/mK]
$\dot{m}$: mass flow rate [kg/s]
N : numbe of tube row [-]
NTU : number of transfer units [-]
P_f : fin pitch [m]
P_l : longitudinal tube pitch [m]
Pr : Prandtl number
P_t : transverse tube pitch [m]
Re_D : Reynolds number based on tube O.D. ($=(\rho V_{max} D)/\mu$)
t : thickness [m]
T : temperature [K]
U : overall heat transfer coefficient [W/m^2K]
V : air velocity [m/s]

Greek symbols

ΔP : pressure drop [Pa]
ε : effectiveness [-]
μ : dynamic viscosity [kg/ms]
η : fin efficiency [-]
η_o : surface efficiency [-]
ρ : density [kg/m^3]
σ : contraction coefficient [-]

Subscripts

a : air
c : fin collar or cross-section

† Corresponding author
Tel.: +82-32-770-8420; fax: +82-32-770-8410
E-mail address: knh0001@incheon.ac.kr

d : dry surface
D : diameter or diffusion
f : fin
i : inside
m : mean
max : maximum
o : outside
r : tube inside
t : tube wall
w : wet surface or water

1. Introduction

Fin-and-tube heat exchangers are extensively used as evaporators of household or commercial air-conditioning units due to structural and manufacturing simplicity. When the fin surface temperature is lower than the dew-point temperature of the incoming air, the moisture is condensed on the fin surface. The condensed moisture releases latent heat of condensation. The wet surface heat transfer consists of the latent heat transfer and the sensible heat transfer. Traditionally, the thermal performance of wet surface has been expressed as a wet surface heat transfer coefficient. The reduction of the wet surface heat transfer coefficient from measured parameters requires heat and mass transfer analysis. Depending on the heat and mass transfer models, the reduced heat transfer coefficients could be significantly different.

The wet surface heat and mass transfer models have been studied by Kim et al.[1] They compared single and dual potential heat and mass transfer models, and showed that the reduced wet heat transfer coefficients were independent of the relative humidity when single potential model was used. The single potential model assumes that the heat and mass transfer is driven by one single potential-enthalpy. In this method, the wet heat transfer coefficient is obtained from the total heat transfer (which includes both latent heat transfer and sensible heat transfer). This model has been recommended by ARI.[2] In the dual potential model, the sensible heat transfer is assumed to be driven by the temperature difference, and the latent heat transfer is assumed to be driven by the humidity difference. In this method, the wet heat transfer coefficient is obtained from the sensible heat alone. This model was proposed by McQuiston.[3] Kim et al.[1] also showed that enthalpy-based fin efficiency model yielded relative-humidity-independent fin efficiencies. When humidity-based fin efficiency model was used, resultant fin efficiencies were strongly dependent on the relative humidity. The enthalpy-based fin efficiency model assumes that the heat and mass transfer between air and fin is driven by a enthalpy difference. This model is in line with the single potential model. In the humidity-based model, the latent heat transfer is linked with the sensible heat transfer through a humidity-temperature relationship. The enthalpy model has been recommended by ARI, and the humidity model was proposed by McQuiston.[3]

The literature shows contradictory trends for the relative magnitude of the wet surface heat transfer coefficients (h_w) and the dry surface heat transfer coefficients (h_d). Existing studies are summarized in Table 1. McQuiston[4] tested four row plain fin samples, and reported that h_d was larger than h_w for P_f>3.175 mm. For the smaller fin pitches, h_d was approximately the same as h_w. McQuiston[4] used the dual-potential model for the heat and mass transfer analysis, and the humidity model for the fin efficiency calculation. Wang et al.[5] tested plain fin heat exchangers of 2, 4 and 6 row configuration, and reported that h_d was approximately the same as h_w. They used the single-potential model for the heat and mass transfer analysis, and the enthalpy model for the fin efficiency calculation. Additional data on wave fin configuration[6-9] shown in Table 1 show contradictory trends, probably due to the different heat and mass transfer, and fin efficiency models.

Several correlations to predict heat transfer

Table 1 Previous studies on wet surface heat transfer of fin-and-tube heat exchangers

Investigators	Heat and mass transfer	Wet fin efficiency	Fin shape	Row	Fin pitch [mm]	Result
McQuiston[4]	Dual	Humidity	Plain	4	1.81~6.35	$h_d > h_w$ ($P_f > 3.17$ mm) $h_d \cong h_w$ ($P_f \leq 3.17$ mm)
Wang et al.[5]	Single	Enthalpy	Plain	2, 4, 6	1.82~3.2	$h_d \cong h_w$
Eckels and Rabas[6]	Single	Enthalpy	Wavy	3	1.97~3.13	$h_w > h_d$
Mirth et al.[7]	Single	Enthalpy	Wavy	4, 8	1.61~3.2	$h_d \cong h_w$
Hong and Webb[8]	Dual	Humidity (Wu & Bong modification)	Wavy Lanced Louver	2, 3	1.49~2.12	$h_d > h_w$
Kim et al.[9]	Single	Enthalpy	Wavy slit	2, 3	1.59~2.12	$h_d \cong h_w$

coefficients and friction factors of plain finned-tube heat exchangers have been developed. They include Wang et al.,[10] Kim et al.,[11] Gray and Webb[12] for the dry surface, and McQuiston[13] and Wang et al.[14] for the wet surface. McQuiston[13] devloped correlations based on his four-row sample data. Different correlations were developed depending on the wet surface characteristics (droplet or film). Wang et al.[14] tested 2, 4 ,6 row samples, and developed correlations based on the test data.

In this study, nine samples having different fin pitches and rows were tested at dry and wet surface conditions. For the wet surface heat transfer coefficient, single potential model was used for the heat and mass transfer analysis, and enthalpy-based model was used for the fin efficiency evaluation following the suggestion by Kim et al.[1] Figure 1 shows the schematic drawing of the plain fin samples tested in this study.

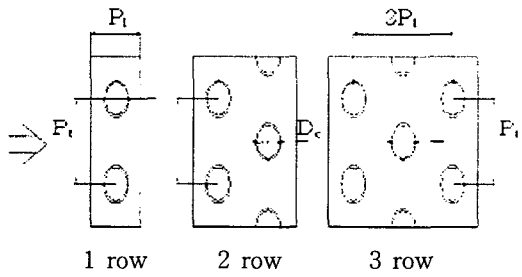

Fig. 1 Shape of the plain fin.

2. Test apparatus and methods

Geometric details of the samples are listed in Table 2. Nine samples having three different

Table 2 Geometric details of heat exchanger samples

Sample no.	D_c [mm]	Fin shape [mm]	P_t [mm]	P_l [mm]	P_f [mm]	t_f [mm]	N
1	7.3	plain	21	12.5	1.49	0.115	1
2	7.3	plain	21	12.5	1.34	0.115	1
3	7.3	plain	21	12.5	1.21	0.115	1
4	7.3	plain	21	12.5	1.49	0.115	2
5	7.3	plain	21	12.5	1.34	0.115	2
6	7.3	plain	21	12.5	1.21	0.115	2
7	7.3	plain	21	12.5	1.49	0.115	3
8	7.3	plain	21	12.5	1.34	0.115	3
9	7.3	plain	21	12.5	1.21	0.115	3

fin pitches (1.21, 1.34, 1.49 mm) and three different rows (1, 2, 3 row) were tested. All the samples had same tube O.D. (D_c=7.3 mm), tube pitches (P_t=21.0 mm, P_l=12.5 mm). The height of the sample was 252 mm, and the width was 400 mm. The fin surface was hydrophilic-coated to facilitate the condensate drainage.

A schematic drawing of the apparatus is shown in Fig. 2. It consists of a suction-type wind tunnel, water circulation and control units, and a data acquisition system. The apparatus is situated in a constant temperature and humidity chamber. The airside inlet condition of the heat exchanger is maintained by controlling the chamber temperature and humidity. Dry and wet bulb temperatures in the inlet and the outlet are measured by the sampling method as suggested in ASHRAE Standard 41.1.[15] A diffusion baffle is installed behind the test sample to mix the outlet air. The water-side inlet condition is maintained by regulating the flow rate and inlet temperature of the constant temperature bath situated outside of the chamber. Both the air and the water temperatures

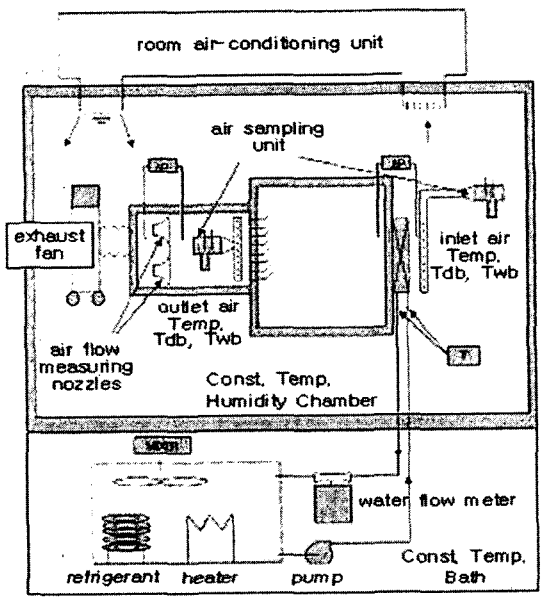

Fig. 2 Schematic drawing of the experimental setup.

are measured by pre-calibrated RTDs (Pt-100Ω sensors). Their accuracies are ±0.1℃. The water flow rate is measured by a positive displacement type flow meter, whose accuracy is ±0.0015 liter/s. The airside pressure drop across the heat exchanger is measured using a differential pressure transducer. The air flow rate is measured using a nozzle pressure difference according to ASHRAE Standard 41.2.[16] The accuracy of the differential pressure transducers is ±1.0 Pa.

The chamber temperature was maintained at 27℃ with 60% RH for wet surface tests, and 21℃ with 50% RH for dry surface tests. The water inlet temperature was maintained at 6℃ for wet tests, and at 60℃ for dry tests. Experiments were conducted varying the frontal air velocity from 0.75 m/s to 2.5 m/s.

The energy balance between the air-side and the tube-side was within ±3%. The discrepancy increased as the air velocity decreased. All the data signals were collected and converted by a data acquisition system (a hybrid recorder). The data were then transmitted to a personal computer for further manipulation. An uncertainty analysis was conducted following ASHRAE Standard 41.5,[17] and the results are listed in Table 3. The major uncertainty on the friction factor was the uncertainty of the differential pressure measurement (±10%), and the major uncertainty affecting the heat transfer coefficient (or j factor) was that of the tube-side heat transfer coefficient (±10%). The uncertainties decreased as the Reynolds number increased.

Table 3 Experimental errors

Parameter	Max. uncertainties
Temperature	±1.0℃
Differential pressure	±1.0 Pa
Water flow rate	$\pm 1.5\times10^{-6}$ m^3/s
Re_{D_c}	±2%
f	±10%
j	±12%

3. Data reduction

3.1 Dry surface

The data reduction details are provided by Kim et al.,[1] and short summary is provided here. For the present cross-counter circuits, the ε-NTU relationship is[18]

$$UA = \{(\dot{m}c_p)_{air}\mathrm{NTU}_2\} \tag{1}$$

$$\mathrm{NTU}_2 = -2\ln(1-K) \tag{2}$$

Here, K is obtained from

$$\frac{K}{2}+\left(1-\frac{K}{2}\right)\exp(2KR)=\frac{1}{1-RP} \quad (2\,\text{row}) \tag{3}$$

$$K\left[1-\frac{K}{4}-RK\left(1-\frac{K}{2}\right)\right]\exp(KR)+\left(1-\frac{K}{2}\right)^2\exp(3KR)=\frac{1}{1-RP} \quad (3\,\text{row}) \tag{4}$$

$$R=\frac{T_{r,in}-T_{r,out}}{T_{air,in}-T_{air,out}} \tag{5}$$

$$P=\frac{T_{air,out}-T_{air,in}}{T_{r,in}-T_{air,out}} \tag{6}$$

For a 1-row configuration, cross-flow ε-NTU relationship is used. The air-side heat transfer coefficient is obtained from Eq. (7).

$$\frac{1}{\eta_o h_o A_o}=\frac{1}{UA}-\frac{1}{h_i A_i}-\frac{t}{kA_t} \tag{7}$$

The tube-side heat transfer coefficient is obtained from appropriate correlations. For the present smooth tube, Gnielinski[19] correlation was used. The surface efficiency η_o in Eq. (7) is obtained from

$$\eta_o = 1-\frac{A_f}{A_o}(1-\eta) \tag{8}$$

The fin efficiency is obtained from Schmidt[20] equation. The heat transfer coefficient is expressed as the j-factor.

$$\mathrm{Re}_D=\frac{\rho_a V_{\max} D_c}{\mu_a} \tag{9}$$

$$j=\frac{h_o}{\rho_a V_{\max} c_{pa}}\mathrm{Pr}_a^{2/3} \tag{10}$$

The friction factor is obtained from

$$f=\frac{A_c}{A_o}\frac{\rho_m}{\rho_{in}}\left[\frac{2\Delta P\rho_{in}}{(\rho_m V_{\max})^2}-(1+\sigma^2)\left(\frac{\rho_{in}}{\rho_{out}}-1\right)\right] \tag{11}$$

3.2 Wet surface

Kim et al.[1] provide data reduction details for the wet surface heat transfer coefficient, and short summary is provided here. When enthalpy potential is the driving force, the definition of ε and NTU is different from those of the temperature driving system, and they are provided by Kim et al.[1] For the cross-counter configuration of this study,

$$UA = \dot{m}_a\mathrm{NTU}_2 \tag{12}$$

$$\mathrm{NTU}_2 = -2\ln(1-K) \tag{13}$$

The K equations [Eqs. (3) and (4)] remain the same. However, R and P [Eqs. (5) and (6)] are re-defined using enthalpies instead of temperatures.

$$R=\frac{i_{r,in}-i_{r,out}}{i_{a,out}-i_{a,in}} \tag{14}$$

$$P=\frac{i_{a,out}-i_{a,in}}{i_{r,in}-i_{a,in}} \tag{15}$$

In Eqs. (14) and (15), i_r is the saturated air enthalpy at the tube-side water temperature. Once UA is obtained from an appropriate ε-NTU relation, the sensible heat transfer coefficient is calculated from Eq. (16).

$$\frac{b_{w,m}}{\eta_o h_w A_o} = \frac{1}{UA} - \frac{b_r}{h_i A_i} - \frac{b_t t}{kA_t} \quad (16)$$

Here, b_r, b_t, $b_{w,m}$ are the saturated-air enthalpy-temperature slope at the water, tube wall, and water film temperature, respectively. The wet surface fin efficiency is obtained from

$$\phi = \frac{\tanh(mL)}{mL} \quad (17)$$

$$m^2 = \frac{h_{eff} P}{k_f A_c} \cong \frac{2h_{eff}}{k_f t} \quad (18)$$

$$h_{eff} \equiv \frac{hm''}{c_{p_{ma}}} \quad (19)$$

$$m'' \equiv \left[\frac{di}{dT}\right]_{T_{s,m}} \quad (20)$$

4. Experimental results and discussions

Figures 3 to 5 show the dry and wet surface j and f factors. For the dry surface, the effect of fin pitch is not significant for one- and two-row configuration. For the three-row configuration, at low Reynolds number, the heat transfer coefficient slightly increases as the fin pitch increases. Many previous investigators[5,21] also reported that the effect of fin pitch on the heat transfer coefficient and the friction factor is not significant.

The wet surface heat transfer coefficients are compared with those of the dry surface in Figs. 3 to 5. Similar to the dry surface case, the effect of fin pitch is not significant. The wet surface heat transfer coefficients are approximately the same as those of the dry surface, except for the one row configuration. For the one row configuration, the dry surface heat transfer coefficients are approximately 30% larger than those of the wet surface. The wet surface friction factors are approximately 30% larger than those of the dry surface for all configurations.

Figure 6 illustrates the row effect of the dry surface. All three samples have the same fin

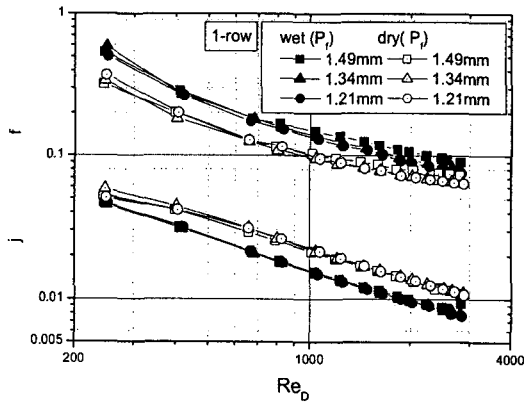

Fig. 3 Effect of fin pitch on the dry and wet surface j and f factor (one-row).

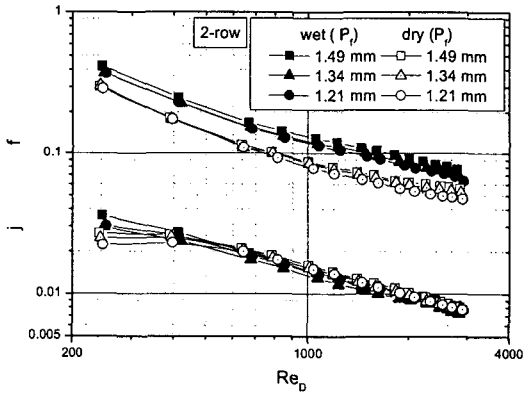

Fig. 4 Effect of fin pitch on the dry and wet surface j and f factor (two-row).

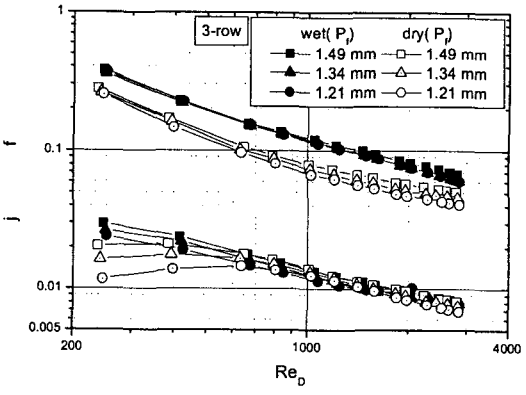

Fig. 5 Effect of fin pitch on the dry and wet surface j and f factor (three-row).

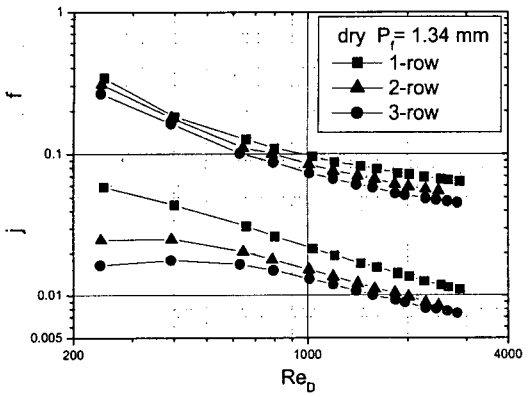

Fig. 6 Effect of tube row on the dry surface j and f factors for 1.34 mm fin pitch.

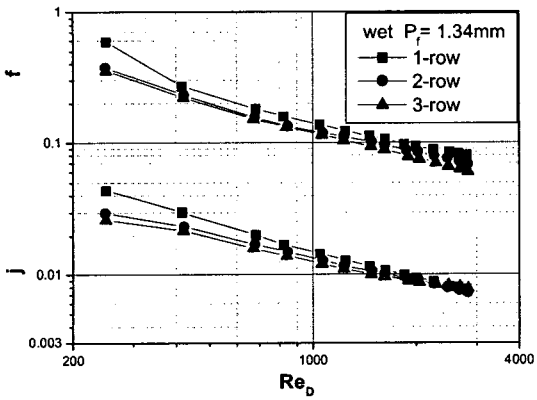

Fig. 7 Effect of tube row on the wet surface j and f factors for 1.34 mm fin pitch.

pitch (P_f=1.34 mm). The heat transfer coefficient decreases as the number of row increases. The difference decreases as the Reynolds number increases. These trends are typical for finned-tube heat exchangers, and may be attributed to the thin boundary-layer on the fin surface for small row samples. The friction factor also decrease as the number of row increases.

Figure 7 shows the wet surface j and f factors for different tube rows at 1.34 mm fin pitch. Similar trend to the dry surface – increase of j and f factors for decreasing row number – is noticed. As the Reynolds number increases, the row effect on the heat transfer coefficient diminishes.

The literature reveals several wet surface data. McQuiston[4] tested four-row samples, and reported that the heat transfer coefficient decreased as the fin pitch increased. For the 6.4 mm fin pitch, the wet surface heat transfer coefficient was larger than that of the dry surface. However, the trend was reversed for 2.5 mm fin pitch. Eckels and Rabas[6] tested three-row samples, and reported that both the heat transfer coefficient and the friction factor were larger for the wet surface compared to the dry surface. Idem et al.[23] tested four-row circular finned-tube samples, and reported that the wet surface heat transfer coefficient was larger than that of the dry surface. Wang et al.[5] tested 2, 4, 6-row samples, and reported that the wet surface heat transfer coefficient is approximately the same as that of the dry surface. They also reported that the effect of fin pitch was negligible, and the effect of number of row was smaller for the wet surface. Wang et al.'s results are in close agreement with those of the present study. Wang et al.[5] used the same data reduction method as those used in the present study.

One notable thing of the present data is that the drop-off of the j factor at low Reynolds numbers, which is typical for the dry surface j factor, is not observed for the wet surface. Similar trend was reported by Wang et al.[5] They explained that, for the wet surface, condensates were hung on the tubes, which enhanced the downstream heat transfer.

4.1 Correlations

The present data were compared with existing correlations – Gray and Webb,[12] Kim et al.,[11] Wang et al.[10] for the dry surface, and McQuiston,[13] Wang et al.[14] for the wet surface. Figure 8 compares the dry surface data with the correlations. For the j factor, Kim et al.[11] correlation predicts the data best. The

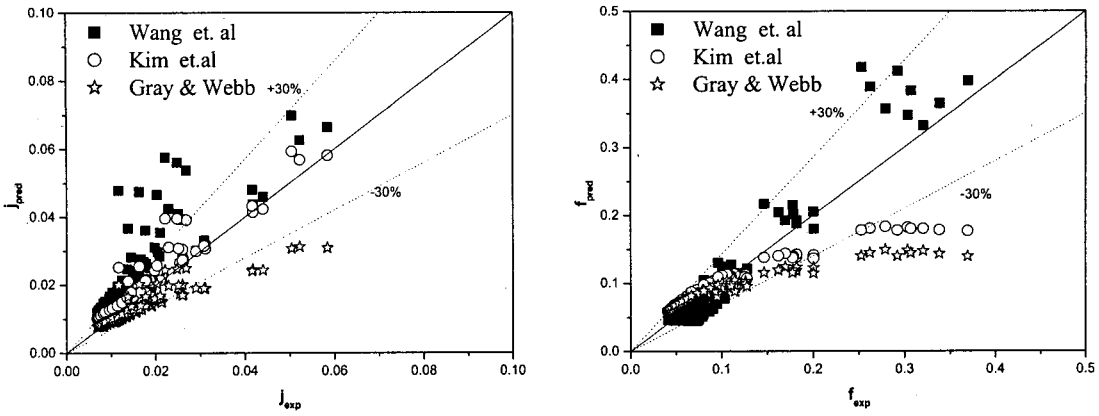

(a) j factor (b) f factor

Fig. 8 The present dry surface j and f data compared with existing correlations.

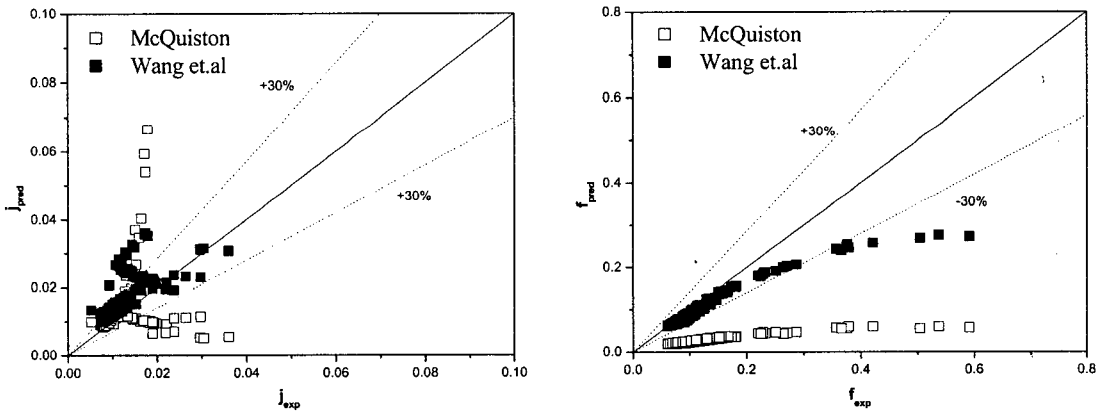

(a) j factor (b) f factor

Fig. 9 The present wet surface j and f data compared with existing correlations.

data are overpredicted by Wang et al.[10] correlation, and underpredicted by Gray and Webb[12] correlation. The friction factors are well predicted by Wang et al.[10] correlation. Kim et al.[11] and Gray and Webb[12] correlation underpredicts the large friction data. Figure 9 compares the wet surface data with the correlations. Wang et al.[14] correlation adequately predicts the j and f factors. McQuiston[13] correlation overpredicts or underpredicts the data.

5. Conclusions

In this study, dry and wet surface pressure drop and heat transfer characteristics of heat exchangers having plain fins were investigated. Nine samples having different fin pitches (1.21, 1.34, 1.49 mm) and rows (1, 2, 3 row) were tested.

(1) The effect of the fin pitch on the heat transfer coefficient and the friction factor is not significant.

(2) The heat transfer coefficient and the friction factor decrease as the number of tube row increases.

(3) For one-row configuration, the wet surface heat transfer coefficient is smaller than that of the dry surface. However, the difference decreases as the number of row increases.

(4) The drop-off of the j factor curve at low Reynolds numbers does not occur for the wet surface.

(5) The wet surface friction factor is approximately 30% larger than the dry surface friction factor.

(6) The present dry surface heat transfer coefficient is well predicted by Kim et al.[11] correlation. The wet surface heat transfer is well predicted by Wang et al.[14] correlation.

References

1. Kim, N.-H., Oh, W.-K., Cho, J.-P., Park, W.-Y. and Baek, Y., 2003, Data reduction on the air-side heat transfer coefficients of heat exchangers under dehumidifying conditions, Korean Journal of Air-Conditioning and Refrigeration, Vol. 15, No. 1, pp. 73-85.
2. ARI 410-81, Standard for forced-circulation air-cooling and air-heating coils, American Refrigeration Institute.
3. McQuiston, F. C., 1975, Fin efficiency with combined heat and mass transfer, ASHRAE Trans., Vol. 81, No. 1, pp. 350-355.
4. McQuiston, F. C., 1978, Heat, mass and momentum transfer data for five plate-fin-tube surfaces, ASHRAE Trans., Vol. 84, Part 1, pp. 266-293.
5. Wang, C.-C., Hsieh, Y.-C. and Lin, Y.-T., 1997, Performance of plate finned tube heat exchangers under dehumidifying conditions, J. Heat Transfer, Vol. 119, pp. 109-117.
6. Eckels, P. W. and Rabas, T. J., 1987, Dehumidification: on the correlation of wet and dry transport process in plate finned-tube heat exchangers, J. Heat Transfer, Vol. 109, pp. 575-582.
7. Mirth, D. R., Ramadhyani, S. and Hittle, D. C., 1993, Thermal performance of chilled water cooling coils at low water velocities, ASHRAE Trans., Vol. 99, Pt. 1, pp. 43-53.
8. Hong, K. and Webb, R. L., 1999, Performance of dehumidifying heat exchangers with and without wetting coatings, J. Heat Transfer, Vol. 121, pp. 1018-1026.
9. Kim, N.-H., Kim, J.-S., Yun, J.-H., Peck, J.-H., Lee, S.-K., Nam, S.-B. and Kwon, H.-J., 1997, Wet surface performance test of fin-and-tube heat exchangers with slit-wavy fin, Korean Journal of Air-Conditioning and Refrigeration, Vol. 9, No. 2, pp. 153-162.
10. Wang, C.-C., Chi, K.-Y. and Chang, C.-J., 2000, Heat transfer and friction characteristics of plain fin-and-tube heat exchangers, Part II: correlation, Int. J. Heat Mass Trans., Vol. 43, pp. 2693-2700.
11. Kim, N.-H., Youn, B. and Webb, R. L., 1999, Air-side heat transfer and friction correlations for plain fin-and-tube heat exchangers with staggered tube arrangements, J. Heat Transfer, Vol. 121, pp. 662-667.
12. Gray, D. L. and Webb, R. L., 1986, Heat transfer and friction correlations for plate fin-and-tube heat exchangers having plain fins, Proceedings of the 9th International Heat Transfer Conference, Taylor & Francis, London, San Francisco, pp. 2745-2750.
13. McQuiston, F. C., 1978, Correlation of heat, mass and momentum transport coefficients for plate-fin-tube heat transfer surfaces with staggered tubes, ASHRAE Transactions, Part 1, Vol. 84, pp. 294-309.
14. Wang, C.-C., Hsieh, Y.-C. and Lin, Y.-T., 1997, Performance of plate finned tube heat exchangers under dehumidifying conditions, J. of Heat Transfer, Vol. 119, pp. 109-117.
15. ASHRAE Standard 41.1, 1986, Standard method for temperature measurement, ASHRAE.
16. ASHRAE Standard 41.2, 1986, Standard method for laboratory air-flow measurement, ASHRAE.
17. ASHRAE Standard 41.5, 1986, Standard measurement guide, engineering analysis of experimental data, ASHRAE.
18. Taborek, J., 1998, F and θ charts for cross-flow arrangements, in Heat Transfer Enhancement of Heat Exchangers, Eds., S.

Kakac, A. E. Bergles, F. Mayinger and H. Yuncu, Kluwer Academic Press, pp. 141-162.
19. Gnielinski, V., 1976, New equations for heat and mass transfer in turbulent pipe flows, Int. Chem. Eng., Vol. 16, pp. 359-368.
20. Schmidt, T. E., 1949, Heat trasfer calculations for extended surfaces, J. ASRE, Refrigeration Engineering, Vol. 4, pp. 351-357.
21. Rich, D. G., 1973, The effect of fin spacing on the heat transfer and friction preformance of multi-row, plate fin-and-tube heat exchangers, ASHRAE Transactions, Part 2, Vol. 79, pp. 137-145.
22. Rich, D. G., 1975, The effect of number of tube rows on the heat transfer performance of smooth plate-fin-tube heat exchangers, ASHRAE Trans., Vol. 81, Part 1, pp. 307-317.
23. Idem, S. A., Jacobi, A. M. and Goldschmidt, V. W., 1990, Heat transfer characterization of a finned-tube heat exchanger (with and without condensation), Journal of Heat Transfer, Vol. 112, pp. 64-70.